Title

Can Leaf Spectroscopy Predict Leaf and Forest Traits Along a Peruvian Tropical Forest Elevation Gradient?

Journal

Journal of Geophysical Research Biogeosciences, 122(11)

ISSN

2169-8953

Authors

Doughty, Christopher E
Santos-Andrade, PE
Goldsmith, GR
et al.

Publication Date

2017-11-01

DOI

10.1002/2017jg003883

Peer reviewed

Can Leaf Spectroscopy Predict Leaf and Forest Traits Along a Peruvian Tropical Forest Elevation Gradient?

Christopher E. Doughty[1], P. E. Santos-Andrade[2], G. R. Goldsmith[3], B. Blonder[4], A. Shenkin[4], L. P. Bentley[5], C. Chavana-Bryant[4], W. Huaraca-Huasco[2,4], S. Díaz[6], N. Salinas[2,7], B. J. Enquist[8,9], R. Martin[10], G. P. Asner[10], and Y. Malhi[4]

[1] SICCS, Northern Arizona University, Flagstaff, AZ, USA, [2] Departamento de Ecologia, Universidad Nacional San Antonio Abad del Cusco, Cusco, Perú, [3] Ecosystem Fluxes Group, Laboratory for Atmospheric Chemistry, Paul Scherrer Institute, Villigen, Switzerland, [4] Environmental Change Institute, School of Geography and the Environment, University of Oxford, Oxford, UK, [5] Department of Biology, Sonoma State University, Rohnert Park, CA, USA, [6] Instituto Multidisciplinario de Biología Vegetal (IMBIV), CONICET and Universidad Nacional de Córdoba, Córdoba, Argentina, [7] Seccion Quimica, Pontificia Universidad Catolica del Peru, Lima, Peru, [8] Department of Ecology and Evolutionary Biology, University of Arizona, Tucson, AZ, USA, [9] Santa Fe Institute, Santa Fe, New Mexico, USA, [10]Department of Global Ecology, Carnegie Institution for Science, Stanford, CA, USA

Correspondence to: C. E. Doughty, chris.doughty@nau.edu

Abstract

High-resolution spectroscopy can be used to measure leaf chemical and structural traits. Such leaf traits are often highly correlated to other traits, such as photosynthesis, through the leaf economics spectrum. We measured VNIR (visible-near infrared) leaf reflectance (400–1,075 nm) of sunlit and shaded leaves in ~150 dominant species across ten, 1 ha plots along a 3,300 m elevation gradient in Peru (on 4,284 individual leaves). We used partial least squares (PLS) regression to compare leaf reflectance to chemical traits, such as nitrogen and phosphorus, structural traits, including leaf mass per area (LMA), branch wood density and leaf venation, and “higher-level” traits such as leaf photosynthetic capacity, leaf water repellency, and woody growth rates. Empirical models using leaf reflectance predicted leaf N and LMA (r^2 > 30% and %RMSE < 30%), weakly predicted leaf venation, photosynthesis, and branch density (r^2 between 10 and 35% and %RMSE between 10% and 65%), and did not predict leaf water repellency or woody growth rates (r^2<5%). Prediction of higher-level traits such as photosynthesis and branch density is likely due to these traits correlations with LMA, a trait readily predicted with leaf spectroscopy.

1 Introduction

The distribution of traits within individual trees and between species may help indicate resilience of forests to future climate change (Diaz & Cabido, 1997; Lavorel & Garnier, 2002; Westoby & Wright, 2006) and enable the estimation of ecosystem fluxes (Enquist et al., 2015). Understanding these trait distributions on a regional scale could therefore improve predictions of

carbon cycling in tropical forests. Many leaf traits are associated with and can be predicted by other leaf traits. The most famous example of this is the leaf economics spectrum, which found that 82% of all variation in photosynthetic capacity (A_{mass}), leaf mass per area (LMA), and nitrogen content (N_{mass}) across species from a variety of global biomes, lay along the first principal axis in three-trait space on a log-log scale (Wright et al., 2004). Other studies found that LMA could predict mass-based assimilation and respiration rates and that leaf life span could predict many other traits (Poorter & Bongers, 2006). Woody growth rates can also be predicted by traits. For example, seed mass, LMA, wood density, and tree height have been predicted to be low for light-demanding species with rapid growth and mortality and high for shade-tolerant species with slow growth and mortality (Wright et al., 2010). Low LMA reflects the “live fast and die young” strategy because it expresses a trade-off within the leaf itself between the energetic cost of leaf construction and the light captured per area (Diaz et al., 2016; Poorter et al., 2009).

Foliar chemical and morphological traits, such as nitrogen (N) concentration and LMA, can be estimated remotely using high-resolution spectroscopy (either VNIR (400–1,100) or VSWIR (400–2,500 nm) spectral properties) in combination with the partial least squares (PLS) regression technique (Richardson et al., 2002; Serbin et al., 2014). Remote measurement of leaf chemistry and structure is possible because leaf spectral reflectance signatures vary based on the concentrations of N, chlorophylls, carotenoids, lignin, cellulose, leaf mass per unit area (LMA), soluble carbon (C), and water (Curran, 1989a, 1989b; Sims & Gamon, 2002; Smith, Kelly, et al., 2003; Smith, Martin, et al., 2003). For example, a leaf's N concentrations are associated with wavelengths absorbed by chlorophyll *a* and *b* in the visible part of the spectrum (400–700 nm), the spectral red edge (700–760 nm), and proteins in the shortwave infrared (1,300–2,500 nm) (Gitelson & Merzlyak, 1997; Kokaly, 2001; Smith, Martin, et al., 2003). In the shortwave infrared (SWIR; 700–1,300 nm), structures such as palisade cell density are important controls on the spectral reflectance because of the very low effective photon penetration distance at these wavelengths. LMA can now be accurately measured using high-spectral-resolution sampling techniques at both the leaf (one nm bandwidth) (Curran, 1989a, 1989b; Jacquemoud et al., 2009; Kokaly et al., 2009), canopy and landscape scales (at 10 nm bandwidth) (Asner et al., 2016, 2015). Even chemicals not directly expressed in the spectrum, such as phosphorus (P), base cations (calcium (Ca), potassium (K), and magnesium (Mg)) and other micronutrients, show relationships with the spectrum, possibly through a stoichiometric relationships with other chemicals (Ustin et al., 2004, 2006).

Another goal of imaging spectroscopy is to quantify photosynthetic capacity and woody growth capacity of forests, since woody growth and carbon sequestration can impact global climate by modifying atmospheric CO_2 concentrations. The relationship between leaf properties such as LMA and

woody growth rates could enable the prediction of mean woody growth rates via a leaf's spectral signature (Poorter et al., 2009). Year to year variation in growth rates is dominated by environmental variation, but long-term growth strategies are possibly associated with leaf traits (Diaz et al., 2016, Wright et al., 2004). Therefore, leaf traits associated with growth strategies could allow spectroscopy to predict these growth trends. Previous work has shown that leaf spectral properties can predict traits or attributes beyond leaf chemistry or structure. For instance, leaf age has been predicted with high-resolution leaf spectroscopy (400–2,500 nm) and leaf age is not directly expressed in a leaf's spectral signature (Chavana-Bryant et al., 2017). Previous work has also shown that other leaf properties such as photosynthetic capacity that may not directly influence leaf spectral signatures can also be predicted with spectroscopy (Doughty et al., 2011).

Spectroscopy may also provide a useful field estimate of many difficult-to-measure plant traits associated with a leaf's carbon uptake and hydraulic strategies indirectly through correlations. In principle, spectroscopy could potentially be used to quickly estimate leaf vein density (VD), which is often correlated to photosynthetic capacity and conductance (Brodribb et al., 2007). Likewise, spectroscopy could potentially predict structural traits related to hydrophobic leaf waxes interacting with a water droplet (a data set we use in this paper called leaf water repellency and more fully described in Goldsmith et al., 2016). Such traits currently require difficult or time-consuming laboratory analyses to measure. Can we instead use leaf spectral properties to rapidly estimate such leaf traits in the field or use remote sensing of the spectral properties to better predict carbon and hydraulic strategies?

In this study, we ask whether leaf spectroscopy can predict forest functional traits and higher-level properties by focusing on a 3,300 m elevation gradient in Peru with some of the highest levels of species, trait, and environmental diversity in the world. A previous study on a nearby elevation gradient demonstrated how sunlit leaf spectral patterns change with elevation and used leaf spectral properties to accurately predict 21 leaf chemical and physical traits (Asner, Martin, et al., 2014). It also found interspecific variation in spectral and chemical traits dominated over intraspecific variation among sun leaves of canopy trees. However, that study did not address shaded foliage, which constitutes the majority of canopy leaves, nor traits not directly associated with foliar chemical properties. Without shade leaf spectral data it is unknown how whole canopy spectra will vary since shaded leaf spectra have a strong influence on total canopy reflectance in the NIR wavelengths. For this paper, our main question of interest is the following:

Can VNIR reflectance of sun and shade leaves predict tree traits and higher-level properties such as woody growth along a tropical forest elevation gradient?

We also ask the following specific questions:

Do shade leaves show equally high levels of interspecific variation in leaf reflectance to sun leaves?

Can VNIR spectral properties (400–1,075 nm) predict leaf chemical and structural traits as well as full VSWIR spectral properties (400–2,500 nm)? Can underside spectral signature predict traits as well as the top-of-leaf?

Is there a relationship between leaf spectral properties and nonfoliar traits such as photosynthesis, woody NPP, and wood density? What are the structural and chemical drivers of these relationships?

2 Materials and Methods

2.1 Field Sites

These measurements were made as part of the CHAMBASA (CHallenging Attempt to Measure Biotic Attributes along the Slopes of the Andes) campaign from April to November 2013 along an elevation gradient (from 3,500 m to 220 m elevation) in the Peruvian Amazon (Table S1 in the supporting information). The plots are part of a long-term research effort coordinated by the Andes Biodiversity Ecosystems Research Group (ABERG, http://www.andesconservation.org) and are part of the ForestPlots (https://www.forestplots.net/) and Global Ecosystems Monitoring Network (http://gem.tropicalforests.ox.ac.uk/projects/aberg). Plots were established between 2003 and 2013 in areas with minimal evidence of human disturbance. Within each plot, all stems ≥10 cm diameter at breast height are tagged and identified to species level. There is a negative linear relationship in the gradient between mean annual temperature and elevation with a mean annual temperature of 24.4°C in the warmest lowland Amazonian site and 9.0°C at the Amazonian treeline in the Andes. Mean annual precipitation varies from 1,560 to 5,302 mm yr^{-1} along the elevation gradient. Soils at elevations >600 m are composed of relatively high-fertility Inceptisols and Entisols. In the lowlands (<600 m above sea level), soils vary among Ultisols on low-fertility terra firme clay substrates and Inceptisols on inactive high-fertility floodplains. We describe characteristics of the plots in Table S1. All data in this paper can be found in a data repository with the following DOI: https://ora.ox.ac.uk/objects/uuid:4101e249-3cf5-443f-9c29-9204604c667b.

2.2 Leaf Collections Sampling Strategy

In each 1 ha plot (N = 10 plots), we sampled the most abundant species as determined through basal area weighting (enough species generally to cover 80% of the plot's basal area, although in the diverse lowland plots only 60–70% of plot basal area were sampled). For each species, we sampled the five (three in the lowlands) largest trees (based on diameter at breast height (DBH)) and tree climbers with extended tree pruners removed one branch grown in sun and one grown in shade conditions. These branches were

quickly recut underwater to restore hydraulic conductivity. On each of these branches, we choose five random leaves. These five leaves were each sampled for photosynthesis, leaf spectral properties (generally measured within 1 h of being cut), and Leaf Mass Area (LMA—leaves scanned for area immediately after collection using a digital 476 scanner (Canon LiDE 110) and oven-dried at 72°C until constant weight reached) and leaf water repellency (see below for methods) later that day. On three of the five leaves, we later measured leaf chemistry (% N, C, and P). Total phosphorus content was determined using persulfate oxidation followed by the acid molybdate technique, and phosphorus concentration was then measured colorimetrically with a spectrophotometer (Thermo Scientific Genesys20, USA). Carbon and nitrogen content were measured on a continuous-flow gas-ratio mass spectrometer (Finnigan Delta PlusXL) coupled to an elemental analyzer (Costech). On approximately one leaf per branch, we measured leaf venation. The rest of the leaves from the branch were used for a bulk chemical analysis following the protocol outlined below.

2.3 Leaf Photosynthesis

We used a portable gas exchange system (LI 6400, Li-Cor Biosciences, Lincoln, NE, USA) to measure light-saturated leaf photosynthesis (A_{sat}; 1,200 µmol m^{-2} s^{-1} PPFD, 400 ppm CO_2, at the MAT of the plot) and maximum photosynthesis (A_{max}; 1,200 µmol m^{-2} s^{-1} PPFD, 1,000 ppm CO_2, at the MAT of the plot). Photosynthetic capacity in most tropical leaves saturate above light levels of 1,200⁻µmol m^{-2} s^{-1} PPFD (Doughty & Goulden, 2008). Most physiological measurements were collected between 07:00 and 14:00 local time, and branches were cut from tree between 06:00 and 13:00 local time.

2.4 Vein Density

We prepared a slide of each leaf's venation network by chemically clearing and staining pressed dried leaf material (Pérez-Harguindeguy et al., 2013). We then photographed the leaf using an Olympus SZX-12 microscope setup for trans-illumination. We then traced all veins within a polygonal region of interest of each image (mean area 36 ± 23 s.d. mm^2). We calculated vein density (VD) in MATLAB by dividing the total length of the skeletonized traced veins by the total area of the region of interest, then correcting for any shrinkage of the leaf imposed by drying. For further information see the Methods of Blonder et al. (2017) and Figure 1.

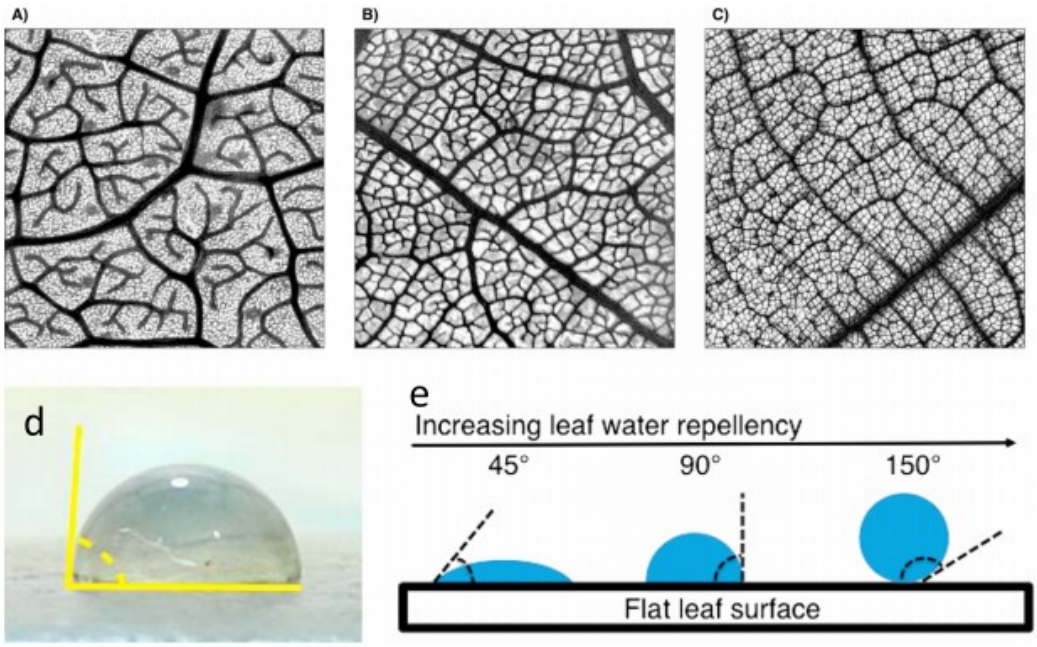

Figure 1. Vein density is highly variable between species. Example venation networks are shown for (a) *Cavendishia bracteata* (Ericaceae), 6.8 mm^{-1}; (b) *Clethra cuneata* (Clethraceae), 14.3 mm^{-1}; (c) *Pourouma bicolor* (Urticaceae), 24.9 mm^{-1}. (d) Leaf water repellency is measured as the contact angle of a droplet of water on a leaf surface and (e) samples of different measured angles (repeated from Goldsmith et al., 2016).

2.5 Leaf Water Repellency

Each leaf was first secured flat to a horizontal surface. A 5 µl droplet of water was then placed on the adaxial side of the leaf using a micropipette, and a photograph was taken of the horizontal profile of the droplet using a digital camera. We removed epiphylls by hand or using a tissue when necessary. We measured the contact angle (θ) as the angle between the line tangent at the edge of the water droplet and the horizontal line of contact of the water droplet on the leaf surface (Figure 1). Higher leaf water repellency has a larger contact angle (Rosado & Holder, 2013). We outlined the water droplet as an ellipse to help more accurately identifying the tangent prior to determining contact angle. Analysis was conducted in ImageJ v1.47 (U. S. National Institutes of Health, Bethesda, Maryland). For further details see Goldsmith et al. (2016) and Figure 1.

2.6 Bulk Leaf Chemistry

Leaves from branches not selected for photosynthesis measurements were used for a bulk chemical analysis with methodology detailed in Asner, Anderson, et al. (2014) and in documents available on the Carnegie Spectranomics website (http://spectranomics.ciw.edu) (Table S2). Foliage was dried and ground in a 20 mesh Wiley mill, and concentrations of Phosphorus (P), Calcium (Ca), Potassium (K), Magnesium (Mg), Boron (B), Iron (Fe), Manganese (Mn), and Zinc (Zn) were measured using coupled plasma spectroscopy (ICP-OES; Therma Jarrel-Ash,Waltham, MA, USA) after microwave digestion (MARSXpress; CEM, Matthews, NC, USA). We determined carbon fractions of cellulose, lignin, hemicellulose, and soluble C

(composed of amino acids, pectins, simple sugars, starch, and waxes) in 0.5 g of dry ground leaf tissue with sequential digestion in a fiber analyzer (Ankom Technology, Macedon, NY, USA). These results are shown in Table S2.

2.7 Woody NPP and Branch Wood Density

All trees >10 cm DBH at the 10 plots have had periodic census measurements of their DBH. We used the change in DBH during the longest available interval (ranging between 1 and 30 years) to estimate the mean growth rate of that tree. We divided this growth rate by the tree's DBH to estimate a yearly percentage growth rate. For branch wood density, we measured six branch sections per tree (approximately 1 cm in diameter and 5 cm in length). Bark was removed from three of the samples. They were weighed wet, and volume measured by immersing in water and converting weight to volume. The branches were then dried in an oven to a constant weight and reweighed. For further details see Malhi et al. (2017).

2.8 Leaf Spectroscopy

We measured hemispherical reflectance near the midpoint between the main vein (avoiding large primary or secondary veins) and the leaf edge on the top and bottom (Figure S1) surface of five randomly selected leaves within an hour of each branch being cut. We collected the spectra with an ASD Fieldspec Handheld 2 with a fiber optic cable, contact probe which has its own calibrated light source and a leaf clip (Analytical Spectral Devices High Intensity Contact Probe and Leaf Clip, Boulder, Colorado, USA). The spectrometer records 750 bands spanning the 325–1,075 nm wavelength region. Measurements were collected with 136 ms integration time per spectrum. To ensure measurement quality, the spectrometer was optimized after every branch, spectra for every leaf were calibrated for dark current, stray light and white referenced to a calibration panel (Spectralon, Lasphere, Durham, New Hampshire, USA). In each measurement spot (on each side of the leaf) 25 spectra were internally averaged to increase the signal-to-noise ratio of the data.

2.9 Data Processing

We calculated coefficient of variation (CV) of our spectral data as the standard deviation divided by the mean. To predict leaf traits with the spectral information, we used the Partial Least Squares Regression (PLSR) modeling approach (Geladi & Kowalski, 1986; Wold et al., 2001). This approach incorporates the full spectral information within each leaf reflectance measurement versus a single band analysis (Kokaly et al., 2009), thus reducing our large predictor matrix (675 spectral bands—400–1,075 nm) down to a relatively few, uncorrelated latent factors. This approach has been previously demonstrated to yield accurate and consistent results for predicting plant traits within and across vegetation types and ecosystems (Asner & Martin, 2008; Richardson et al., 2002 ; Serbin et al., 2014). To

establish predictive models for chemical, structural and higher-level leaf traits, we used the PLSregress command in Matlab (Matlab, MathWorks Inc., Natick, MA, USA). We avoided overfitting the number of latent factors we used for each analysis by minimizing the mean square error with cross validation (on 70% of the data, and then tested the model on an independent 30% of the data). This process removes one sample from the input data set until we minimize the mean square error. For each trait model, we selected the number of latent vectors by choosing the number that minimized the root-mean-square error (RMSE). To compute the mean square error of prediction, we use K-fold cross validation. To create a completely independent testing data set, we use 70% of our data to calibrate our model and then the remaining 30% to test the accuracy of our model. We evaluated the accuracy of our modeled estimates using two main metrics: r^2 and root-mean-square error (RMSE).

3 Results

Mean visible (400–700 nm) leaf reflectance for all the plots was 0.050 for sun leaves and 0.046 for shade leaves, with greater visible CV in the sun leaves (0.232 versus 0.197). In the NIR (800–1,075 nm), mean leaf reflectance was 0.514 for sun leaves and 0.511 for shade leaves, with similar CV (0.098 versus 0.099) (Table 1 and Figures 2 and 3). There were no differences with elevation when we subtracted sun from shade leaves (Figure 2 insets). Overall significant differences between sun and shade leaves are shown in Figure S1. There were no significant ($P > 0.05$) linear trends in reflectance or CV with elevation (Table 1) in either the visible or the NIR. CV between leaves of the same species (intraspecific variation) was less than CV between species (interspecific variation) in sun leaves (0.25 versus 0.10 maximum CV in the visible) and shade leaves (0.20 versus 0.08 maximum CV in the visible). Interspecific variation peaked in the visible wavelengths (25% CV for sun and 21% CV for shade leaves) (Figure 3).

Table 1

Mean, Standard Deviation (SD), and Mean Coefficient of Variation (CV) for All Spectra Measured in the 10 Plots in the Visible (VIS, 400–700 nm) and the Near Infrared (NIR, 800–1,075 nm) for Both Sun Leaves and Shade Leaves, Respectively

		Sun VIS			Sun NIR			Shade VIS			Shade NIR		
Plot	Elevation (m)	Mean reflectance	SD	CV	Mean reflectance	SD	CV	Mean reflectance	SD	CV	Mean reflectance	SD	CV
Acjanaco 1	3,537	0.052	0.013	0.252	0.501	0.062	0.124	0.046	0.011	0.240	0.503	0.038	0.077
Wayqecha	3,045	0.050	0.012	0.238	0.523	0.056	0.107	0.040	0.004	0.105	0.534	0.114	0.213
Esperanza	2,868	0.052	0.010	0.193	0.524	0.042	0.081	0.050	0.010	0.206	0.506	0.046	0.092
Trocha Union 4	2,719	0.052	0.012	0.233	0.511	0.058	0.114	0.049	0.010	0.211	0.515	0.052	0.101
San Pedro 1	1,713	0.051	0.012	0.233	0.510	0.070	0.138	0.050	0.011	0.221	0.511	0.061	0.119
San Pedro 2	1,494	0.047	0.009	0.202	0.511	0.055	0.109	0.046	0.009	0.190	0.511	0.050	0.099
Pantiacolla 3	859	0.046	0.011	0.237	0.513	0.038	0.075	0.043	0.009	0.203	0.509	0.039	0.077
Pantiacolla 2	595	0.045	0.009	0.201	0.515	0.040	0.078	0.043	0.008	0.179	0.512	0.032	0.062
Tambopata 5	223	0.050	0.012	0.251	0.503	0.032	0.064	0.046	0.009	0.196	0.496	0.030	0.061
Tambopata 6	215	0.052	0.014	0.280	0.527	0.048	0.091	0.049	0.010	0.214	0.511	0.044	0.087
Mean		0.050	0.011	0.232	0.514	0.050	0.098	0.046	0.009	0.197	0.511	0.051	0.099

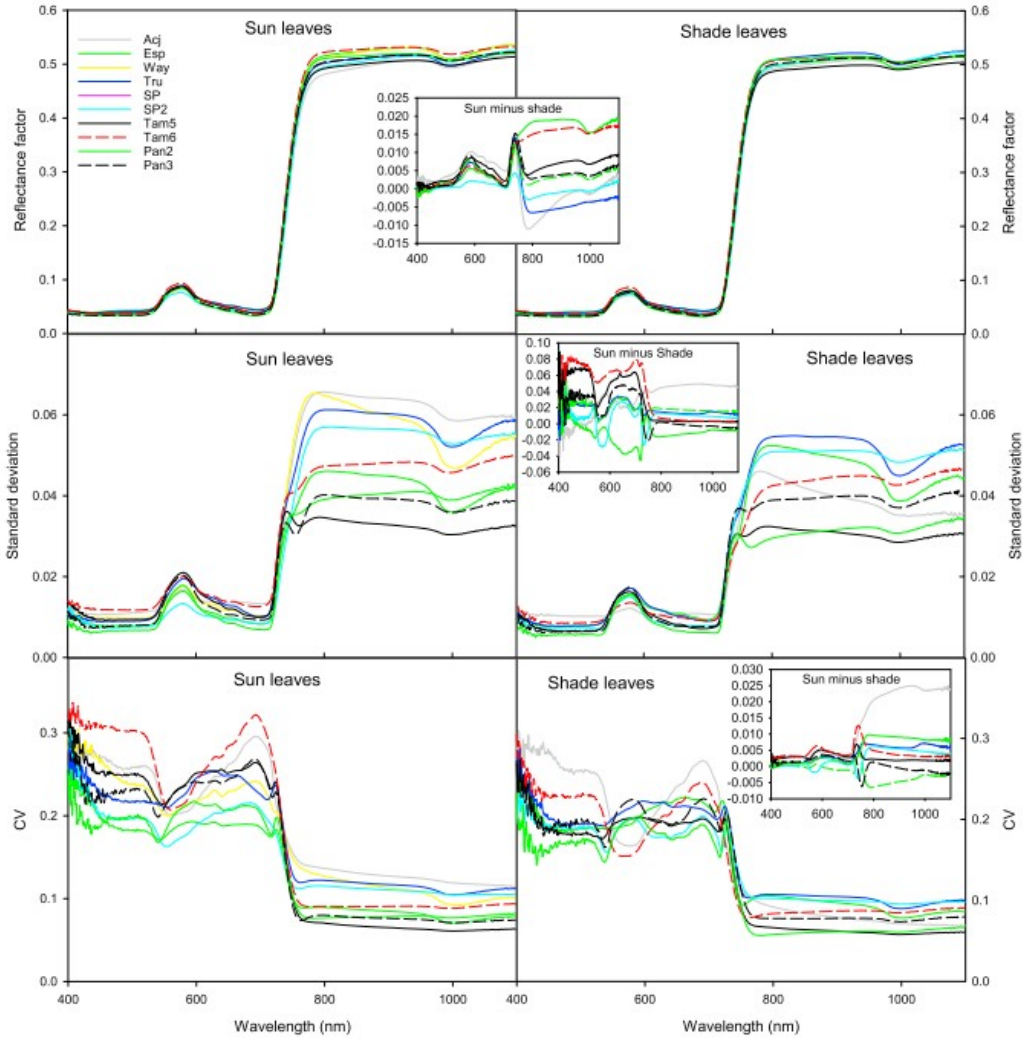

Figure 2. This figure illustrates the mean reflectance properties per research plot (along an elevation gradient). Leaf reflectance (top), standard deviation of this reflectance (middle), and coefficient of variation (plot SD divided by the plot mean) (bottom) for sunlit (left) and shaded (right) leaves. Inset figures are the differences between the sun and shade leaves for reflectance (top), standard deviation (middle), and coefficient of variation (bottom).

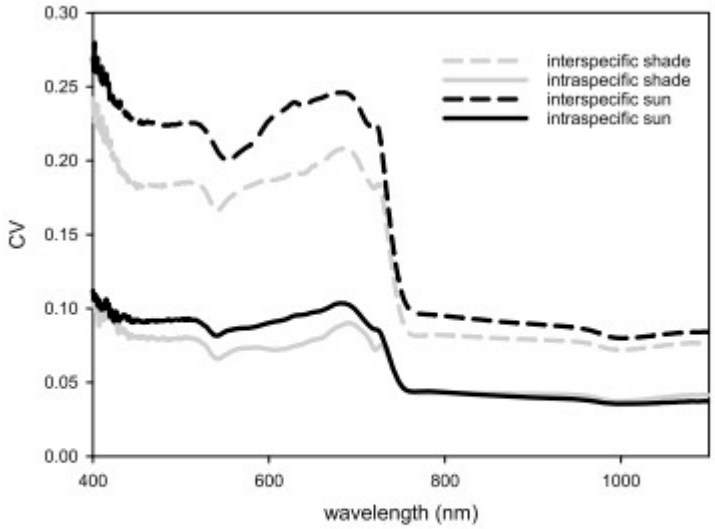

Figure 3. Leaf reflectance interspecific (difference between mean tree spectra) coefficient of variation (dashed lines) (SD/mean) and intraspecific (difference between leaves on the same tree) variation (solid lines) for sunlit (black lines) and shaded (grey lines) leaves.

We then used the PLS regression technique to compare individual leaf spectral characteristics to leaf chemical values for LMA, %N, and %P (Figure 4 and Table 2) measured on the same leaves (results for the PLSR for bulk chemistry are shown in Table S2). The predictions of the empirical models generally matched the measured estimates with high accuracy and precision. The primary principal component weighting demonstrates which regions of the spectra are most important for the empirical model (as measured by deviation away from zero) (Figure 4). LMA had the strongest predicted relationship with an r^2 of 0.76 and a RMSE/mean of 0.27 (Table 2), indicating that leaf spectral characteristics can accurately predict LMA, a finding supported by several other studies (Jacquemoud et al., 2009; Kokaly et al., 2009). As expected, the weightings indicate that the spectral region most important for predicting LMA is in the NIR region. Leaf spectral properties also predicted %N accurately (r^2 = 0.64) and with precision (RMSE/mean = 0.23). The most important spectral regions for %N are in the visible, but especially the red edge, with less spectral importance in the NIR. %P was predicted with an r^2 of 0.35, a RMSE/mean of 0.47 and most spectral information in the visible and the red edge regions.

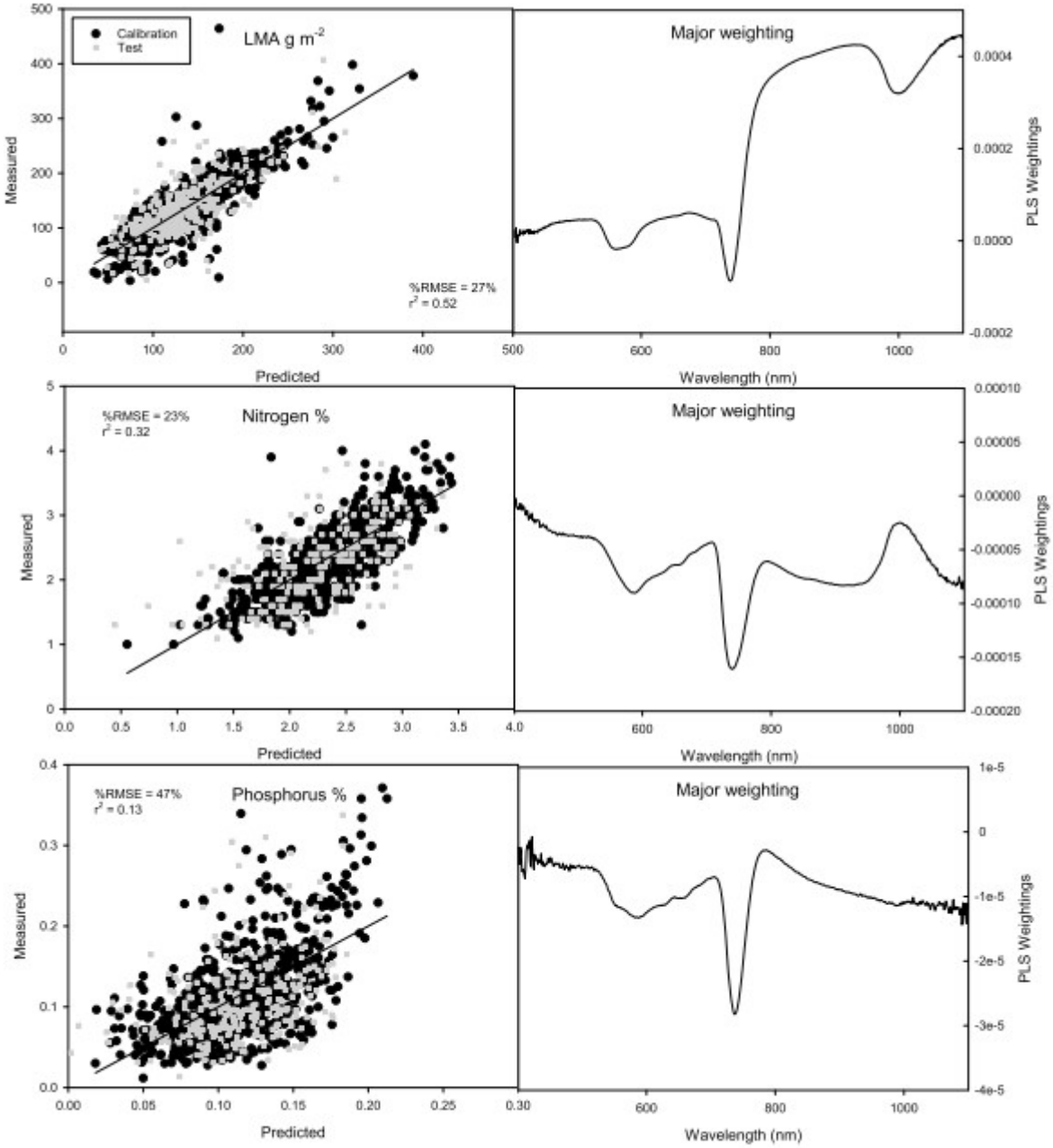

Figure 4. Predicted versus measured values using PLS regressions (left column) and primary principle component for LMA (g m^{-2}), % nitrogen, and % phosphorus (right column).

Table 2
Results of the PLS Regressions for Comparisons of Leaf Level Spectral Properties Versus the Same Leaf Values of LMA, %N, %P, A_{sat}, and A_{max}

	Sun leaves						Shade leaves					
	Mean	N	RMSE	%RMSE	r^2 cal	r^2 test	Mean	*N*	RMSE	%RMSE	r^2 cal	r^2 test
LMA (g m^{-2})	109±44	2601	33.09	0.27	0.76	0.52	136±57	1683	41.90	0.34	0.71	0.55
LMA-abaxial (g m^{-2})	109±44	2601	44.85	0.36	0.74	0.56	136±57	1683	32.26	0.26	0.78	0.54
%N	2.35±0.61	2182	0.53	0.23	0.64	0.32	2.31±0.60	1297	0.52	0.22	0.41	0.28
%P	0.12±0.06	2485	0.05	0.47	0.35	0.13	0.12±0.06	1606	0.06	0.50	0.28	0.06
A_{sat} μmol m^{-2} s^{-1}	6.6±3.0	2601	2.86	0.62	0.17	0.08	5.1±3.6	1683	3.23	0.70	0.24	0.14
A_{max} μmol m^{-2} s^{-1}	10.5±5.1	2601	5.60	0.57	0.14	0.10	8.6±6.2	1683	5.63	0.57	0.18	0.11
Leaf water repellency (deg)	63.4±9.6	331	8.83	0.14	0.07	0.02	64.9±9.1	205	9.11	0.14	0.02	0.01
Vein density—mm^{-1}	14.0±4.7	253	3.76	0.26	0.47	0.32						
Vein area	34.7±25	253	19.99	0.59	0.43	0.25						
Branch wood density—(g cm^{-3})	0.76±0.09	536	0.061	0.078	0.41	0.17	0.75±0.1	371	0.078	0.10	0.66	0.32
Woody growth—(fraction of DBH)	0.02	523	0.03	1.37	0.04	0.01	0.02	523	0.03	1.43	0.01	0.01

Note. We then compared mean branch spectral properties to mean branch or tree values of leaf water repellency, vein density, vein area, branch wood density, and woody growth. The results are presented as mean value (±sd), number of samples (*N*), RMSE, % RMSE (RMSE/mean), r^2 calibration and r^2 test for both sun and shade leaves. The statistics below average 10 separate PLS regression simulations (each independent run varies because the 70% calibration data are randomly selected).

Next, we used leaf reflectance to predict more complex traits (Figure 5). We generally found poorer relationships between these traits than for less complex traits such as leaf chemistry or LMA. Leaf spectra predicted A_{max} (light and CO_2 saturated photosynthesis) with an r^2 of 0.17 and a RMSE/mean of 0.62. The primary principal component for both A_{sat} (light saturated) and A_{max} (light and CO_2 saturated) photosynthesis had peaks in the NIR and the red edge. This is not surprising as %N and LMA have been shown to be related to A_{max} through the leaf economics spectrum (Wright et al., 2004). A_{sat} demonstrated a similar fit with the spectra as A_{max}, with an r^2 of 0.15 and a RMSE/mean of 0.57. Leaf spectra showed a reasonably strong relationship with leaf minor vein density (r^2 of 0.47 and a %RMSE of 0.26 for sun leaves) and leaf vein surface area (r^2 of 0.43 and a %RMSE of 0.59 for sun leaves). The important spectral regions for predicting leaf vein density have peaks in the red edge and in the NIR. Leaf water repellency was not predicted using the spectra possibly because it did not vary much across the elevation gradient, nor did it vary consistently with taxa and there was much unexplained variance (Goldsmith et al., 2016). Results for the PLSR for both sun and shade leaves are detailed in Table 2.

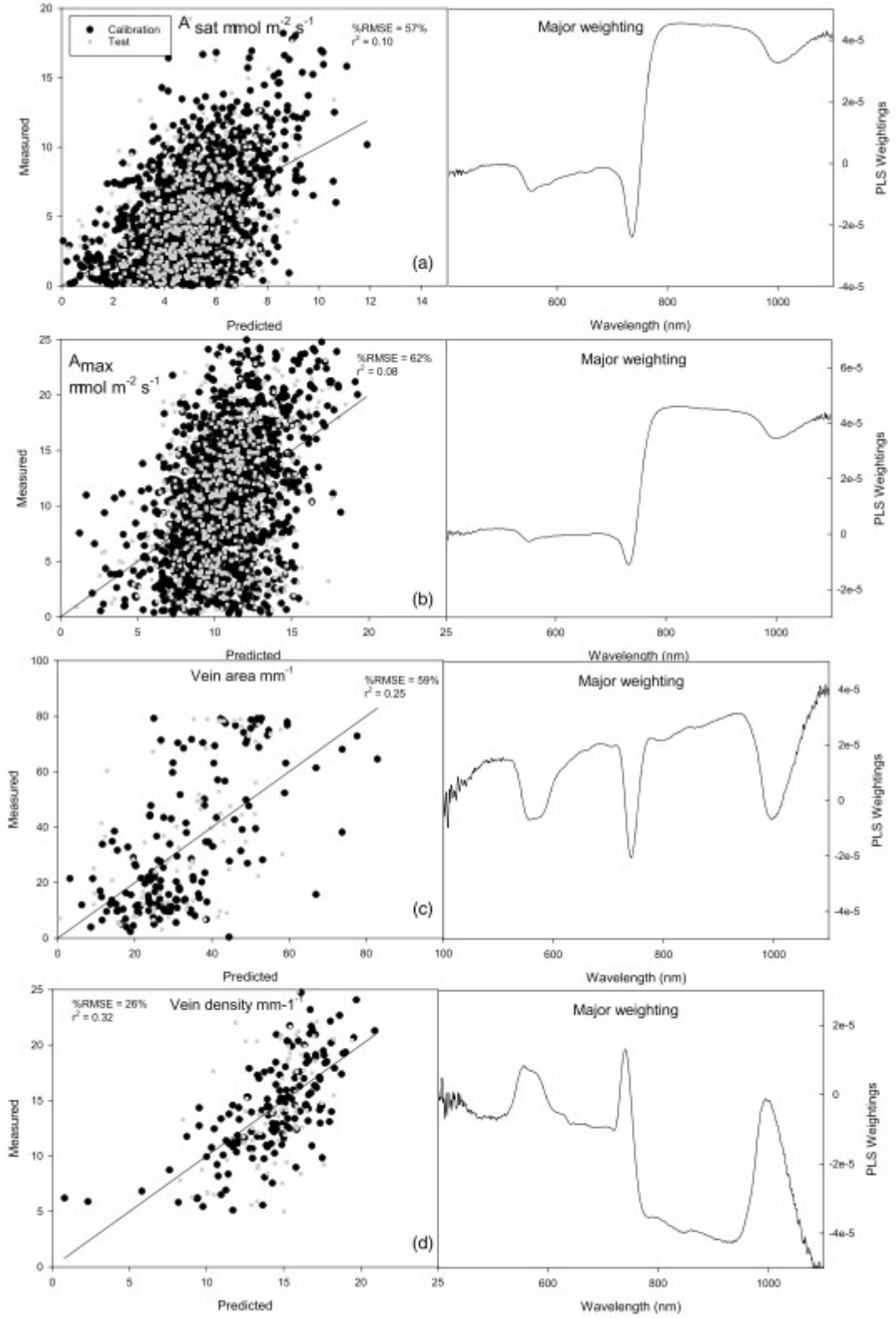

Figure 5. (left) Predicted versus measured values using PLS regressions and (right) primary principle component for (a) A_{sat} (light saturated), (b) A_{max} (light and CO_2 saturated) photosynthesis, (c) leaf vein area mm^{-1} and (d) leaf vein density mm^{-1} for sun leaves.

Finally, we measured whether leaf spectra could be used to predict broader forest characteristics that might be correlated with leaf traits such as branch wood density and mean tree growth rate because long-term growth strategies are possibly associated with leaf traits (Diaz et al., 2016; Wright et al., 2004) (Figure 6). All trees in each plot >10 cm DBH have measured woody NPP using periodic census measurements, and we compare individual tree growth to average leaf reflectance for that tree. We show empirical relationships for sunlit leaves in Figure 6 and for shade leaves in Table 2. Branch wood density demonstrated a strong relationship with the spectra (r^2 of 0.41 and 0.66 and a % RMSE of 0.08 and 0.10 sun/shade). However, woody growth showed no relationship with the spectral signature (r^2 of 0.04 and 0.01 and a % RMSE of 1.37 and 1.43 sun/shade). The important spectral regions for predicting branch wood density are mainly in the NIR, which is similar to leaf structural traits such as LMA.

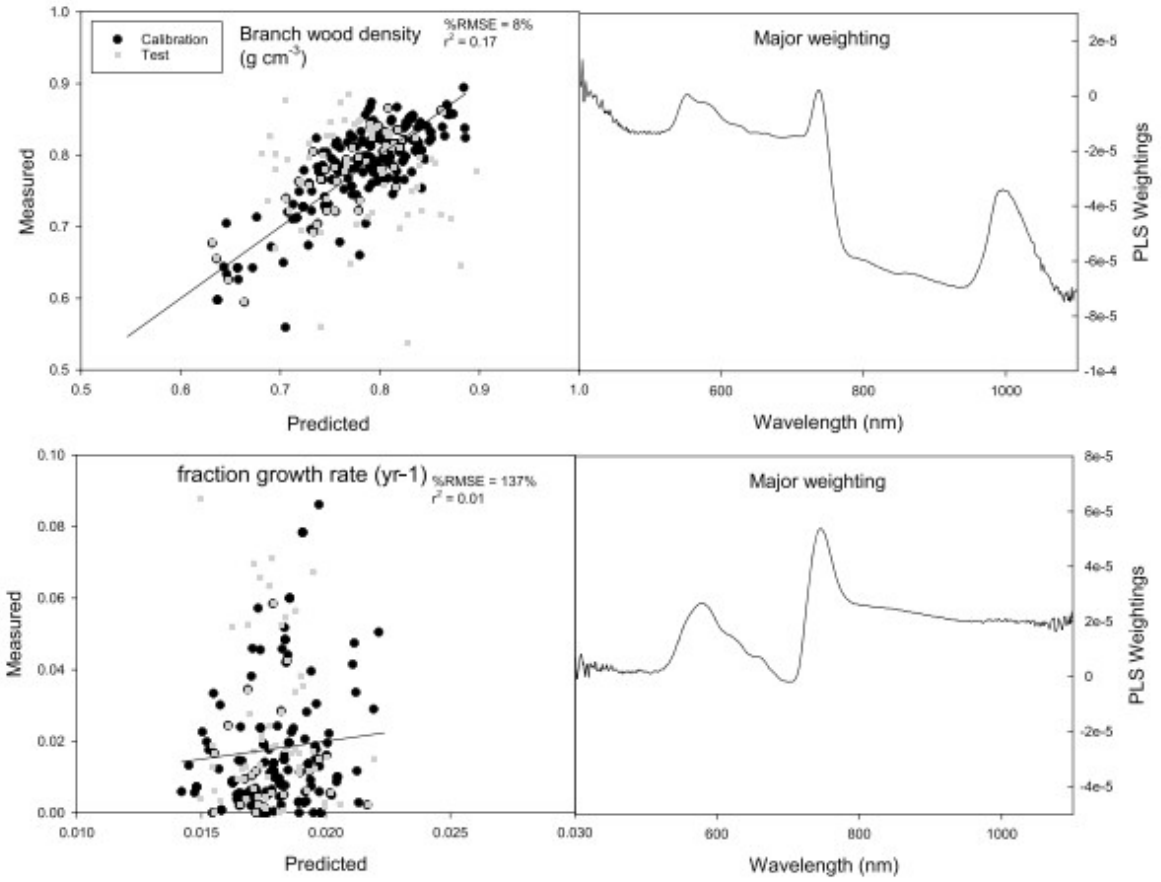

Figure 6. (left) Predicted versus measured PLS regressions for tree averaged leaf spectra versus branch wood density (top) and woody NPP (bottom) for sunlit leaves and (right) the primary principle component weightings for each variable.

To further investigate why there may be relationships between leaf spectra and nonfoliar properties, we then compared mean tree sunlit LMA to branch wood density and mean tree growth rate and found strong significant relationships ($P < 0.005$, but with low variance explained—$r^2 = 0.03$)

between LMA and branch wood density but not mean tree growth rate (Figure 7). This result is similar to the PLS regressions showing predictions of branch wood density using spectra but not mean tree growth rate. The ability of leaf spectral properties to predict branch wood density is likely due to the correlation of these properties to LMA since wood density has been weakly (i.e., r^2 = 0.13 in Wright et al., 2010) correlated with LMA (Diaz et al., 2016; Wright et al., 2010).

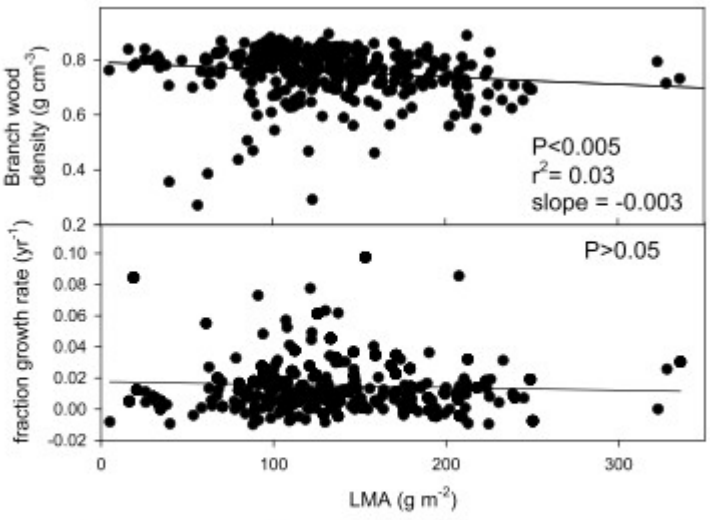

Figure 7. Mean tree averaged sunlit LMA versus (top) branch wood density (g cm^{-3}) and (bottom) mean monthly tree growth rate (yr-1).

4 Discussion

Many previous papers have shown that VNIR reflectance of sun leaves can predict leaf chemistry and structure such as LMA (Curran, 1989a, 1989b; Sims & Gamon, 2002; Smith, Kelly, et al., 2003; Smith, Martin, et al., 2003). However, here we show for the first time that VNIR reflectance of tropical sun and shade leaves can also predict other traits such as leaf venation, photosynthesis, and branch density (explaining between ~10–35% of the variance—Table 2 and SOM) but cannot predict other parameters such as woody growth rates or leaf water repellency. These parameters are not directly estimated from the leaf spectral signature but instead are (weakly) correlated with other leaf chemical and physical traits such as LMA and leaf N (Diaz et al., 2016; Wright et al., 2004) that are directly predicted from leaf spectral properties (Jacquemoud et al., 2009; Kokaly et al., 2009).

Leaf spectroscopy could predict several forest properties not directly expressed in the leaf spectra, such as branch wood density (Figure 6 and Table 2). The PLS weightings of branch wood density are very similar to LMA with most of the signal in the NIR wavelengths. This indicates that the prediction of these parameters (correlation coefficients in Table 2) may actually rest with an accurate prediction of LMA. In other words, Figure 4 demonstrates that leaf spectral properties can strongly predict LMA and

Figure 7 shows that branch wood density and LMA are correlated, which is why there is any predictability of nonfoliar properties by leaf spectral properties. Our prediction of branch wood density using spectroscopy was sufficient to potentially differentiate between large, heavy wood density trees with thick long-lived leaves and smaller, light wood density trees with thin short-lived leaves. This interpretation is reinforced by the significant relationships between LMA and branch wood density (Figure 7). This finding suggests that optical remote sensing could help estimate woody biomass because wood density estimates are key for such estimates. Another example is our empirical models predicting vein density. They do not directly measure veins but rather a cross-sectional area of solute and water relative to mesophyll chemistry that is associated with veins or the fraction of the leaf's volume/biomass that is lignified. Overall, predictions of leaf veins, photosynthesis, and wood density had lower (Table 2) yet still reasonable precision and accuracy comparable to such compounds as tannins, hemicellulose, K, B, Fe, Mn, and Zn (Table S2).

We did not find a relationship between leaf spectral reflectance and mean woody growth rate for a given tree. We had initially hypothesized that there may have been a correlation based on the relationship between LMA and light-demanding pioneer species with rapid growth and mortality (Wright et al., 2010). However, our study was in old growth closed canopy forests, which may have impacted our results. Outside of pioneer species, woody growth rates can be difficult to predict because they are a function of photosynthesis, carbon use efficiency, and the differential allocation of NPP to woody biomass (Doughty et al., 2015, 2014; Malhi et al., 2011, 2015). Such woody NPP growth rates have proven very difficult to accurately estimate even with complicated vegetation models (Cleveland et al., 2015).

Field-based leaf spectroscopy could potentially serve as a replacement for time consuming, lab measurements of traits. For instance, estimation of leaf traits is a time-consuming process that involves manually tracing leaf veins. The RMSE/mean for leaf vein density is <30% with an r^2 of ~50% which can broadly distinguish between low and high values of these traits. This would likely provide a meaningful, though not highly precise, rough field estimate of vein density. As with forest properties such as branch wood density, this may be due to correlations between vein density and the leaf's volume/biomass that is lignified. Thus, the promise of remote sensing for these time-intensive traits may soon be realized.

In this study, empirical models predicting leaf chemical, structural, and photosynthetic parameters were strong overall but less accurate (based on mean r^2) and less precise (based on %RMSE) than those measured in previous studies (Asner & Martin, 2008; Asner et al., 2009; Doughty et al., 2011; Richardson & Reeves, 2005; Serbin et al., 2014). On average, there is a reduction in r^2 of ~0.2–0.3 and a reduction of %RMSE of 20–30% compared with previous studies (specifically comparing Table S2 to Table 2 in Asner, Martin, et al., 2014). For instance, we did find a relationship between A_{sat} and

leaf spectral properties but much weaker (r^2 = 0.14–0.24 versus r^2 = 0.74) than previously observed (Doughty et al., 2011). In both studies, A_{max} was less accurate and precise than A_{sat}. There are several potential reasons for this. First of all, we used spectral bands between 400 and 1,075 nm (VNIR) while previously studies used 400–2,500 nm (VSWIR) (Asner, Martin, et al., 2014). Many chemicals, such as N, are strongly expressed in the near-infrared and SWIR portion of the reflectance spectrum (Kokaly, 2001; Smith, Martin, et al., 2003), a spectral region missing in our study. However, this does not completely explain the difference because a previous study made predictions using less spectral data (400–1,100 nm) and found that predictions of photosynthesis were still strong, with mean RMSE declining by only 10% (from 3.2 to 2.9 when spectral data were reduced from 400–2,500 to 400–1,100 nm) (Doughty et al., 2011). Interestingly, the part of the leaf measured (whether top or bottom of the leaf) does not strongly affect our ability to predict LMA from leaf reflectance spectra (Figure S2).

This study was also unique because we measured shade leaf reflectance along with traits, while few previous studies had measured shade tropical leaf reflectance. Ideally, we could scale our leaf level predictions of higher-level traits to the canopy level with drone, aircraft, or even satellite hyperspectral data. However, to do so, it is important to understand the spectral properties of shade leaves as well since these will be expressed in the NIR of canopy measurements. Our results show equally strong relationships predicting shade leaf traits as they do for predicting sun leaf traits (Table 2).

In addition, our shade leaf data set was also able to resolve another mystery. Interspecific (between species) spectral variability in our data set was higher than in other ecosystems (Asner et al., 2000; Castro-Esau et al., 2004; Roberts et al., 1998). Interspecific variation in leaf reflectance peaked in the visible at ~25% (expressed as coefficients of variation CVs) (Figure 2 and Table 2). These high levels of interspecific variation match a previous campaign, which measured 1,449 canopy tree species and found a maximum CV of 23% in sunlit leaf reflectance (Asner, Martin, et al., 2014). Previous studies hypothesized that interspecific variation was large because they just focused on canopy exposed sun leaves. However, our data show that shaded leaf interspecific variation was still very high but slightly lower than for sunlit leaves, with a mean visible CV of ~21%. Asner, Martin, et al. (2014) hypothesized that interspecific variation in western Amazonian forests dominates over intraspecific variation in this region because the upper canopy foliage is much drier and less susceptible to epiphylls (they estimated epiphylls are present in 9% of the cases in sufficient quantities to affect reflectance), herbivory, and other factors that may increase intraspecific variation in leaf spectral signatures (Asner, Martin, et al., 2014; Vourlitis et al., 2008). However, we show that shade leaves, which are generally more susceptible to epiphylls, also have high levels of interspecific variation compared to intraspecific variation (~0.03 CV lower than the sun

leaves). This indicates that phylogenetic expression in the spectra occurs at the whole canopy-volume scale, a finding reflected in recent work on sunlit versus shade leaves and the chemistry of 21 different compounds. This increases the likelihood that our method could successfully scale to the canopy level.

The western Amazon may have uniquely high levels of interspecific spectral variability. This high spectral diversity may be an intrinsic function of high biological diversity in tropical forests and due to the evolution of high chemical defense levels in response to host-specific pest and pathogen pressure (Asner, Martin, et al., 2014). These high levels of spectral diversity may enable us to use remote sensing to estimate 10–35% of the variation in important forest properties such as photosynthesis and wood density. This accuracy and precision may only allow a binary type detection process distinguishing between low and high values. However, we hypothesize that accuracy and precision will only improve when using the VSWIR instead of just the VNIR and when scaled to the canopy level, as canopy spectroscopy may amplify the leaf-level chemical and physiological signals via the process of effective photon penetration depth (EPPD; (Asner, 2008). Next steps are to test predictions of higher-level traits with high-resolution aircraft systems, such as the Carnegie Airborne Observatory (Asner et al., 2012), or possibly even satellites (Lee et al., 2015). If such systems show similar results to those seen at the leaf level, then we could greatly improve understanding of tropical forests.

Acknowledgments

This work is a product of the Global Ecosystems Monitoring (GEM) network (gem.tropicalforests.ox.ac.uk), the Andes Biodiversity and Ecosystems Research Group ABERG (andesresearch.org), the Amazon Forest Inventory Network RAINFOR (www.rainfor.org), and the Carnegie Spectranomics Project (spectranomics.carnegiescience.edu) research consortia. The field campaign was funded a grant to Y. M. from the UK Natural Environment Research Council (grant NE/J023418/1), with additional support from European Research Council advanced investigator grants GEM -TRAITS (321131), T -FORCES (291585), and a John D. and Catherine T. MacArthur Foundation grant to G. P. A. We thank the Servicio Nacional de Áreas Naturales Protegidas por el Estado (SERNANP) and personnel of Manu and Tambopata National Parks for logistical assistance and permission to work in the protected areas. We also thank the Explorers' Inn and the Pontifical Catholic University of Peru, as well as ACCA. We thank Eric Cosio (Pontifical Catholic University of Peru) for his assistance with research permissions and sample analysis and storage. Taxonomic work at Carnegie Institution was helped by Raul Tupayachi, Felipe Sinca, and Nestor Jaramillo. B. B. was supported by a U.S. National Science Foundation graduate research fellowship and doctoral dissertation improvement grant DEB -1209287, as well as a UK Natural Environment Research Council independent research fellowship NE/M019160/1. G. P. A. and the Spectranomics team were supported by the

endowment of the Carnegie Institution for Science and a grant from the National Science Foundation (DEB -1146206). S. D. was partially supported by a Visiting Professorship Grant from the Leverhulme Trust, UK. Y. M. was also supported by the Jackson Foundation. G. R. G. was supported by funding from the European Community's Seventh Framework Program (FP7/2007-2013) under grant agreement number 290605 (COFUND: PSI-FELLOW). C. E. D. received funding from the John Fell Fund and a Google Earth Engine award. All data in this paper can be found in a data repository with the following DOI: https://ora.ox.ac.uk/objects/uuid:4101e249-3cf5-443f-9c29-9204604c667b. Parts of the data are under embargo through January 2018. Code is available at https://github.com/cdoughty99/JGR_Spectroscopy. C. E. D. wrote the paper with contributions from G. P. A., B. B., P. E. S. A., G. R. G., and C. C. B. PESA and C. E. D. collected the spectral data. P. E. S. A., A. S., L. B., G. G., B. B., W. H. H., N. S., B. E., R. M., G. P. A., and Y. M. provided data. C. E. D. analyzed the data. The field study was funded by grants to Y. M. and G. P. A.

References

Asner, G. P. (2008). Hyperspectral remote sensing of canopy chemistry, physiology and diversity in tropical rainforests. In M. Kalacska & G. A. Sanchez-Azofeifa (Eds.), *Hyperspectral remote sensing of tropical and subtropical forests*. Taylor and Francis Group.

Asner, G. P., Anderson, C. B., Martin, R. E., Knapp, D. E., Tupayachi, R., Sinca, F., & Malhi, Y. (2014). Landscape-scale changes in forest structure and functional traits along an Andes-to-Amazon elevation gradient. *Biogeosciences*, 11(3), 843– 856. https://doi.org/10.5194/bg-11-843-2014

Asner, G. P., Anderson, C. B., Martin, R. E., Tupayachi, R., Knapp, D. E., & Sinca, F. (2015). Landscape biogeochemistry reflected in shifting distributions of chemical traits in the Amazon forest canopy. *Nature Geoscience*, 8(7), 567– 573. https://doi.org/10.1038/NGEO2443

Asner, G. P., Knapp, D. E., Anderson, C. B., Martin, R. E., & Vaughn, N. (2016). Large-scale climatic and geophysical controls on the leaf economics spectrum. *Proceedings of the National Academy of Sciences of the United States of America*, 113(28), E4043– E4051. https://doi.org/10.1073/pnas.1604863113

Asner, G. P., Knapp, D. E., Boardman, J., Green, R. O., Kennedy-Bowdoin, T., Eastwood, M., … Field, C. B. (2012). Carnegie Airborne Observatory-2: Increasing science data dimensionality via high-fidelity multi-sensor fusion. *Remote Sensing of Environment*, 124, 454– 465. https://doi.org/10.1016/j.rse.2012.06.012

Asner, G. P., & Martin, R. E. (2008). Spectral and chemical analysis of tropical forests: Scaling from leaf to canopy levels. *Remote Sensing of Environment*, 112(10), 3958– 3970. https://doi.org/10.1016/j.rse.2008.07.003

Asner, G. P., Martin, R. E., Carranza-Jimenez, L., Sinca, F., Tupayachi, R., Anderson, C. B., & Martinez, P. (2014). Functional and biological diversity of foliar spectra in tree canopies throughout the Andes to Amazon region. *The New Phytologist*, 204(1), 127– 139. https://doi.org/10.1111/nph.12895

Asner, G. P., Martin, R. E., Ford, A. J., Metcalfe, D. J., & Liddell, M. J. (2009). Leaf chemical and spectral diversity in Australian tropical forests. *Ecological Applications*, 19(1), 236– 253. https://doi.org/10.1890/08-0023.1

Asner, C., Wessman, A., Bateson, C. A., & Privette, J. L. (2000). Impact of tissue, canopy, and landscape factors on the hyperspectral reflectance variability of arid ecosystems. *Remote Sensing of Environment*, 74(1), 69–84. https://doi.org/10.1016/S0034-4257(00)00124-3

Blonder, B., Salinas, N., Patrick Bentley, L., Shenkin, A., Chambi Porroa, P. O., Valdez Tejeira, Y., … Malhi, Y. (2017). Predicting trait-environment relationships for venation networks along an Andes-Amazon elevation gradient. *Ecology*, 98(5), 1239– 1255. https://doi.org/10.1002/ecy.1747

Brodribb, T. J., Feild, T. S., & Jordan, G. J. (2007). Leaf maximum photosynthetic rate and venation are linked by hydraulics(1[W][OA]). *Plant Physiology*, 144(4), 1890– 1898. https://doi.org/10.1104/pp.107.101352

Castro-Esau, K. L., Sanchez-Azofeifa, G. A., & Caelli, T. (2004). Discrimination of lianas and trees with leaf-level hyperspectral data. *Remote Sensing of Environment*, 90(3), 353– 372. https://doi.org/10.1016/j.rse.2004.01.013

Chavana-Bryant, C., Malhi, Y., Wu, J., Asner, G. P., Anastasiou, A., Enquist, B. J., … Gerard, F. F. (2017). Leaf aging of Amazonian canopy trees as revealed by spectral and physiochemical measurements. *New Phytologist*, 214(3), 1049– 1063. https://doi.org/10.1111/nph.13853

Cleveland, C. C., Taylor, P., Chadwick, K. D., Dahlin, K., Doughty, C. E., Malhi, Y., … Townsend, A. R. (2015). A comparison of plot-based satellite and Earth system model estimates of tropical forest net primary production. *Global Biogeochemical Cycles*, 29(5), 626– 644. https://doi.org/10.1002/2014GB005022

Curran, P. (1989a). Global change and remote-sensing. *International Journal of Remote Sensing*, 10(9), 1459– 1460. https://doi.org/10.1080/01431168908903982

Curran, P. J. (1989b). Remote-sensing of foliar chemistry. *Remote Sensing of Environment*, 30(3), 271– 278. https://doi.org/10.1016/0034-4257(89)90069-2

Diaz, S., & Cabido, M. (1997). Plant functional types and ecosystem function in relation to global change. *Journal of Vegetation Science*, 8(4), 463– 474. https://doi.org/10.2307/3237198

Diaz, S., Kattge, J., Cornelissen, J. H., Wright, I. J., Lavorel, S., Dray, S., … Gorné, L. D. (2016). The global spectrum of plant form and function. *Nature*, 529(7585), 167– 171. https://doi.org/10.1038/nature16489

Doughty, C. E., Asner, G. P., & Martin, R. E. (2011). Predicting tropical plant physiology from leaf and canopy spectroscopy. *Oecologia*, 165(2), 289– 299. https://doi.org/10.1007/s00442-010-1800-4

Doughty, C. E., & Goulden, M. L. (2008). Seasonal patterns of tropical forest leaf area index and CO_2 exchange. *Journal of Geophysical Research*, 113, G00B06. https://doi.org/10.1029/2007JG000590

Doughty, C. E., Malhi, Y., Araujo-Murakami, A., Metcalfe, D. B., Silva-Espejo, J. E., Arroyo, L., … Ledezma, R. (2014). Allocation trade-offs dominate the response of tropical forest growth to seasonal and interannual drought. *Ecology*, 95(8), 2192– 2201. https://doi.org/10.1890/13-1507.1

Doughty, C. E., Metcalfe, D. B., Girardin, C. A. J., Amezquita, F. F., Durand, L., Huaraca Huasco, W., … Malhi, Y. (2015). Source and sink carbon dynamics and carbon allocation in the Amazon basin. *Global Biogeochemical Cycles*, 29(5), 645– 655. https://doi.org/10.1002/2014GB005028

Enquist, B. J., Norberg, J., Bonser, S. P., Violle, C., Webbjj, C. T., Henderson, A., … Savage, V. M. (2015). Scaling from traits to ecosystems: Developing a general trait driver theory via integrating trait-based and metabolic scaling theories. *Advances in Ecological Research*. https://doi.org/10.1016/bs.aecr.2015.02.001

Geladi, P., & Kowalski, B. R. (1986). Partial least-squares regression—A tutorial. *Analytica Chimica Acta*, 185, 1– 17. https://doi.org/10.1016/0003-2670(86)80028-9

Gitelson, A. A., & Merzlyak, M. N. (1997). Remote estimation of chlorophyll content in higher plant leaves. *International Journal of Remote Sensing*, 18(12), 2691– 2697. https://doi.org/10.1080/014311697217558

Goldsmith, G. R., Bentley, L. P., Shenkin, A., & Malhi, Y. (2016). Variation in leaf wettability traits along a tropical montane elevation gradient. *The New Phytologist*, 214(3), 989– 1001. https://doi.org/10.1111/nph.14121

Jacquemoud, S., Verhoef, W., Baret, F., Bacour, C., Zarco-Tejada, P. J., Asner, C. F., & Ustin, S. L. (2009). PROSPECT plus SAIL models: A review of use for vegetation characterization. *Remote Sensing of Environment*, 113, S56– S66. https://doi.org/10.1016/j.rse.2008.01.026

Kokaly, R. F. (2001). Investigating a physical basis for spectroscopic estimates of leaf nitrogen concentration. *Remote Sensing of Environment*, 75(2), 153– 161. https://doi.org/10.1016/S0034-4257(00)00163-2

Kokaly, R. F., Asner, S., Ollinger, V., Martin, M. E., & Wessman, C. A. (2009). Characterizing canopy biochemistry from imaging spectroscopy and its

application to ecosystem studies. *Remote Sensing of Environment*, 113, S78–S91. https://doi.org/10.1016/j.rse.2008.10.018

Lavorel, S., & Garnier, E. (2002). Predicting changes in community composition and ecosystem functioning from plant traits: Revisiting the Holy Grail. *Functional Ecology*, 16(5), 545– 556. https://doi.org/10.1046/j.1365-2435.2002.00664.x

Lee, C. M., Cable, M. L., Hook, S. J., Green, R. O., Ustin, S. L., Mandl, D. J., & Middleton, E. M. (2015). An introduction to the NASA Hyperspectral InfraRed Imager (HyspIRI) mission and preparatory activities. *Remote Sensing of Environment*, 167, 6– 19. https://doi.org/10.1016/j.rse.2015.06.012

Malhi, Y., Doughty, C., & Galbraith, D. (2011). The allocation of ecosystem net primary productivity in tropical forests. *Philosophical Transactions of the Royal Society B*, 366(1582), 3225– 3245. https://doi.org/10.1098/rstb.2011.0062

Malhi, Y., Doughty, C. E., Goldsmith, G. R., Metcalfe, D. B., Girardin, C. A. J., Marthews, T. R., … Phillips, O. L. (2015). The linkages between photosynthesis, productivity, growth and biomass in lowland Amazonian forests. *Global Change Biology*, 21(6), 2283– 2295. https://doi.org/10.1111/gcb.12859

Malhi, Y., Girardin, C. A. J., Goldsmith, G. R., Doughty, C. E., Salinas, N., Metcalfe, D. B., … Silman, M. (2017). The variation of productivity and its allocation along a tropical elevation gradient: A whole carbon budget perspective. *New Phytologist*, 214(3), 1019– 1032.

Pérez-Harguindeguy, N., Díaz, S., Garnier, E., Lavorel, S., Poorter, H., Jaureguiberry, P., … Gurvich, D. (2013). New handbook for standardised measurement of plant functional traits worldwide. *Australian Journal of Botany*, 61(3), 167– 234. https://doi.org/10.1071/BT12225

Poorter, L., & Bongers, F. (2006). Leaf traits are good predictors of plant performance across 53 rain forest species. *Ecology*, 87(7), 1733– 1743. https://doi.org/10.1890/0012-9658(2006)87%5B1733:LTAGPO%5D2.0.CO;2

Poorter, H., Niinemets, U., Poorter, L., Wright, I. J., & Villar, R. (2009). Causes and consequences of variation in leaf mass per area (LMA): A meta-analysis. *The New Phytologist*, 182(3), 565– 588. https://doi.org/10.1111/j.1469-8137.2009.02830.x

Richardson, A. D., Duigan, S. P., & Berlyn, G. P. (2002). An evaluation of noninvasive methods to estimate foliar chlorophyll content. *The New Phytologist*, 153(1), 185– 194. https://doi.org/10.1046/j.0028-646X.2001.00289.x

Richardson, A. D., & Reeves, J. B. (2005). Quantitative reflectance spectroscopy as an alternative to traditional wet lab analysis of foliar chemistry: Near-infrared and mid-infrared calibrations compared. *Canadian*

Journal of Forest Research, 35(5), 1122– 1130. https://doi.org/10.1139/X05-037

Roberts, D. A., Nelson, B. W., Adams, J. B., & Palmer, F. (1998). Spectral changes with leaf aging in Amazon caatinga. *Trees-Struct Function*, 12(6), 315– 325. https://doi.org/10.1007/s004680050157

Rosado, B. H. P., & Holder, C. D. (2013). The significance of leaf water repellency in ecohydrological research: A review. *Ecohydrology*, 6(1), 150–161. https://doi.org/10.1002/eco.1340

Serbin, S. P., Singh, A., McNeil, B. E., Kingdon, C. C., & Townsend, P. A. (2014). Spectroscopic determination of leaf morphological and biochemical traits for northern temperate and boreal tree species. *Ecological Applications*, 24(7), 1651– 1669. https://doi.org/10.1890/13-2110.1

Sims, D. A., & Gamon, J. A. (2002). Relationships between leaf pigment content and spectral reflectance across a wide range of species, leaf structures and developmental stages. *Remote Sensing of Environment*, 81(2-3), 337– 354. https://doi.org/10.1016/S0034-4257(02)00010-X

Smith, W. K., Kelly, R. D., Welker, J. M., Fahnestock, J. T., Reiners, W. A., & Hunt, E. R. (2003). Leaf-to-aircraft measurements of net CO_2 exchange in a sagebrush steppe ecosystem. *Journal of Geophysical Research*, 108, 4122. https://doi.org/10.1029/2002JD002512

Smith, M. L., Martin, M. E., Plourde, L., & Ollinger, S. V. (2003). Analysis of hyperspectral data for estimation of temperate forest canopy nitrogen concentration: Comparison between an airborne (AVIRIS) and a spaceborne (Hyperion) sensor. *IEEE Transactions on Geoscience and Remote*, 41(6), 1332– 1337. https://doi.org/10.1109/Tgrs.2003.813128

Ustin, S. L., Asner, J. A. G., Huemmrich, K. F., Jacquemoud, S., Schaepman, M., & Zarco-Tejada, P. (2006). Retrieval of quantitative and qualitative information about plant pigment systems from high resolution spectroscopy, 2006. *IEEE International Geoscience and Remote Sensing Symposium*, 1-8, 1996– 1999. https://doi.org/10.1109/Igarss.2006.517

Ustin, S. L., Roberts, D. A., Gamon, J. A., Asner, G. P., & Green, R. O. (2004). Using imaging spectroscopy to study ecosystem processes and properties. *Bioscience*, 54(6), 523– 534. https://doi.org/10.1641/0006-3568(2004)054%5B0523:Uistse%5D2.0.Co;2

Vourlitis, G. L., Nogueira, J. D., Lobo, F. D., Sendall, K. M., de Paulo, S. R., Dias, C. A. A., … de Andrade, N. L. R. (2008). Energy balance and canopy conductance of a tropical semi-deciduous forest of the southern Amazon Basin. *Water Resources Research*, 44, W03412. https://doi.org/10.1029/2006WR005526

Westoby, M., & Wright, I. J. (2006). Land-plant ecology on the basis of functional traits. *Trends in Ecology & Evolution*, 21(5), 261– 268. https://doi.org/10.1016/j.tree.2006.02.004

Wold, S., Sjöström, M., & Eriksson, L. (2001). PLS-regression: A basic tool of chemometrics. *Chemometrics and Intelligent Laboratory Systems*, 58(2), 109– 130. https://doi.org/10.1016/S0169-7439(01)00155-1

Wright, S. J., Kitajima, K., Kraft, N. J., Reich, P. B., Wright, I. J., Bunker, D. E., … Zanne, A. E. (2010). Functional traits and the growth-mortality trade-off in tropical trees. *Ecology*, 91(12), 3664– 3674. https://doi.org/10.1890/09-2335.1

Wright, I. J., Reich, P. B., Westoby, M., Ackerly, D. D., Baruch, Z., Bongers, F., … Villar, R. (2004). The worldwide leaf economics spectrum. *Nature*, 428(6985), 821– 827. https://doi.org/10.1038/nature02403